INNSPUB

Journal of Biodiversity and Environmental Sciences (JBES)
ISSN: 2220-6663 (Print) 2222-3045 (Online)
Vol. 21, No. 6, p. 11-17, 2022
http://www.innspub.net

RESEARCH PAPER OPEN ACCESS

Synthesis and characterization of nanocomposite by using antibacterial activity

N. Daniel Sam[1], CI. Anish[1], G. Sabeena[2], S. Rajaduraipandian[2], SP. Manobala[2], G. Annadurai[*2], M. Jaya Rajan[1]

[1]*Annai Velankanni College, Manonmaniam Sundaranar University, Tholayavattam, India*

[2]*Sri Paramakalyani Centre of Excellence in Environmental Sciences, Manonmaniam Sundaranar University, Alwarkurichi, India*

Article published on December 03, 2022

Key words: Nanocomposite, Characterisation, Antibacterial activity

Abstract

Recently, Cd-TiO_2 Nanocomposite have been synthesized by sol gel methods for the study of the antibacterial activity on Gram positive and Gram negative bacteria by well diffusion method. These prepared Cd-TiO_2 Nanocomposite have been characterized by X-ray diffraction (XRD), Scanning electron microscopy (SEM-EDAX), Ultra Violet Spectroscopy (UV), Fourier Transform Infrared Spectroscopy (FTIR) and Surface Area Analysis (BET). The respective XRD patterns indicate crystalline nature having a rhombohedral structure. The particle size of Cd-TiO_2 nanocomposite in 35nm. SEM images confirm the spherical morphology of the sample. The purity of the synthesized Cd-TiO_2 Nanocomposite have been confirmed from the energy-dispersive X-ray (EDAX) spectra and then C, O, Ti, Cd, Pt element are present in Cd-TiO_2 Nanocomposite. The weight percentage of Cd is 5.8%, Ti is 51.03%, C is 5.13% and O is 31.75% in Cd-TiO_2 Nanocomposite. BET image shows that the major pore size distribution of Cd-TiO2 nanocomposites is ranged from 2.24nm. The Cd-TiO_2 nanocomposite showed that the antibacterial activity when tested against the pathogens only gram negative bacteria such as *Pseodomonous*. The zone of minimum inhibition concentration was measured in a range of 20mm in 25µl and 30mm in 100µl.

***Corresponding Author:** G. Annadurai ✉ gannadurai@msuniv.ac.in

Introduction

The latest development of nanotechnology increases the number of potential applications of synthetic nano-scale materials (Nanopowders, nanocomposites, nanofibers, etc.), the products considered by using sizes below 100nm trendy at smallest one dimension (Giovanni *et al.,* 2015). Metals have been used for centuries as bactericidal agents; silver, copper, gold, titanium, cadmium and zinc have involved particular devotion, each having numerous properties and spectra of activity (Vanaja *et al.,* 2013). Cadmium nanocrystals recently have involved huge attention owing toward their unique size-dependent optical and electrical properties resultant from their quantum confinement effect. Their properties can be adjusted finely by fixing with different suitable material, used for important technological purposes including antibacterial activity (Li *et al.,* 2011; Demir *et al.,* 2012; Qian *et al.,* 2012). Titanium dioxide has numerous crystalline structures which are used in solar cells, air purifier catalysts, photovoltaic materials, gas and humidity sensors and antireflection coatings (Han *et al.,* 2006; Samuela *et al.,* 2005; Chen *et al.,* 2006). Powdered titanium oxide is likewise normally used as a whitener in toothpastes (Malarkodi *et al.,* 2013). The antibacterial, antifungal, and antiviral activities of nanoparticles have remained approximately investigated in evaluation with other metals but, in recent years, only a few authors have reported the antibacterial activity of metal such as cadmium nanocrystals (Zare *et al.,* 2018; Tabatabaee *et al.,* 2013). The development of novel cadmium-based quantum dots or carbon materials shows abundant potential in the treatment and identification of cancer and targeted drug delivery owing to their better size, highly optical fluorescence property, and ease to functionalize the tissue (Rzigalinski *et al.,* 2009)

It is reported that the receptivity of TiO_2 with visible light capacity significantly improved by doping with numerous elements (Umebayashi *et al.*, 2003; Pelaez *et al.,* 2014). In recent years, there has remained growing interest in Cadmium using Titanium Oxide nanocomposite by way of a possible new material for Optical fiber (Fades *et al.,* 1993; Dislich *et al.,* 1993; Pettit *et al.,* 1993). In order to replace other materials, pure and high qualities with uniform crystals of Cadmium with Titanium Oxide nanocomposite of good optical quality are needed. Generally, it has been found that reaction sintering is difficult to control, especially when a chemically homogeneous, single phase product with high purity high density and uniform microstructure is desired. Sol-Gel processing has been investigated extensively as an alternative to conventional processing (Phani *et al.,* 1998). This method involves the controlled hydrolysis of an alkoxide, followed by condensation, which in turn, forms a gel. The structure of the final compound or material is very sensitive to pH, stability of the reactants, amount of water, and impurities. In the present investigation work, we describe the synthesis of Cadmium with Titanium Oxide (Cd-TiO_2) nanocomposite powders using a Sol-Gel technique, which leads to high purity crystalline powders at temperatures lower than solid state reactions. In this work, We have tested the prepared Cadmium with Titanium Oxide (Cd-TiO_2) nanocomposite against these bacteria to study their antibacterial effect against Gram negative and Gram positive bacteria after proper morphological and structural characterization of the prepared sample through Scanning Electron Microscopy (SEM), Fourier Transform Infrared Spectroscopy (FTIR), Ultraviolet Spectroscopy (UV), and X-ray diffraction (XRD).

Materials and method

Chemicals and Materials

Titanium (IV) isopropoxide (TIP, g97.0%), N-dimethylformamide (DMF, g99.8%) and 1-butyl- 3-methylimidazolium hexafluorophosphate (PF6, g97.0%) were purchased from Sigma-Aldrich, Inc. (Milwaukee, WI). The Cadmium Sulphate (g99.8%) and acetonitrile (g99.5%) used in our experiments. All these chemicals were used as received. Deionized water was used throughout the experiments except for in the antibacterial tests, when sterilized H_2O was used.

Preparation of Cd-TiO_2 Nanocomposite Powders

A solution comprising 5 mL of PF6 and 45 mL of DMF was made, in which a desired amount of $CdSO_4$

was dissolved. Titanium (IV) isopropoxide (9.68 mL) was slowly introduced into the solution with vigorous stirring. Deionized H_2O (2.28 mL) was added dropwise to hydrolyze and form a gel. After overnight aging, the gel was washed with acetonitrile repeatedly to remove the entrapped PF6, vacuum-dried at 80 °C, and calcined in air at 600°C for 4 h to produce Cd-TiO_2 nanocomposite powder.

Characterization of Cd-TiO_2 Nanocomposite

The specific surface area (BET) was also determined to analyze the chemical compositions of Cd-TiO_2. To study the crystalline structure, X-ray diffraction (XRD) patterns were recorded on a powder X-ray diffractometer (X'pert Pro). The morphology of Cd-TiO_2 Nanocomposite was examined using a Scanning Electron Microscope (SEM, Model JEOL JEM-2010F) in combination with an energy-dispersive X-ray spectroscopy (EDX) probe for microscopic elemental analysis. Fourier transform infrared (FTIR) spectrometer (BRUKER Vertex-70) was employed for ascertaining the bonds and stretching modes present.

Antibacterial activity

Antibacterial susceptibility testing was carried out by the standard well diffusion method (Azam *et al.,* 2012) against gram negative bacteria such as *Escherichia coli, Pseudomonas, Enterobacter* and gram positive bacteria such as *Staphylococcus aureus, Bacillus subtilis* The bacterial cultures were grown in Nutrient broth media, for 24 h. Then, the wells were filled with a fixed volume of the Cd-TiO_2 nanocomposite and water as a control. The plates were placed in a refrigerator (5-10 min) for successive diffusion, and subsequently, the bacterial strains were incubated at 37°C for 24 h, After the incubation, the diameter of the inhibition zone was determined and recorded. The experiments were performed in triplicate, and therefore, the average diameter of the inhibition zone with its standard deviation was determined.

Result and discussion

X- ray Diffraction

X-ray diffraction (XRD) is used for phase identification where the diffracted intensities are recorded as a function of 2μ. The XRD pattern of the Cd-TiO_2 nanocomposite powder calcinated at 600°C for 4 h has been shown in the Fig. 1. Fig. 1 shows that the particular diffraction peaks at 27.1°, 36.0°, 39.0°, 41.1°, 44.0°, 54.5°, 56.5°, 63.0°, 64.5°, 69.0°. The all peaks of Cd-TiO_2 nanocomposite are indicating the Crystalline size of the phase. On the other hand, sharp and intensive peaks are observed for the sample calcinated at 600°C for 4 h, indicating a higher degree of crystallinity. A weak (JCPDS No. 29-1360) peak was observed in the pure TiO2 sample. Sharp peak represent as (Cd- TiO_2 nanocomposite) Cadmium present from Titanium Oxide nanopowder.

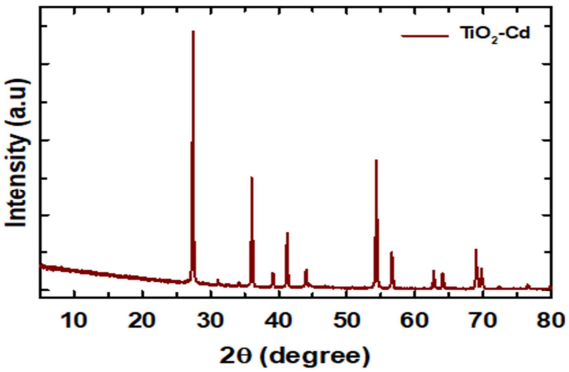

Fig. 1. The XRD image of Cd-TiO_2 Nanocomposite.

For the sample of all the diffraction lines agree with reported values and match with the JCPDS data (card No: 29-277) confirming the formation of rhombohedral structure. The crystallite size is calculated and found to be Scherrer formula applied to the three highest peak such as 27.1°, 36.0°, 54.5° orientation which is the maximum reflection of the rhombohedral structure of Cd-TiO_2 nanocomposite. The particle size of Cd-TiO_2 nanocomposite in 35nm. The increase in Cd loading appears to increase the TiO2 crystallite size in the powders. The actual TiO2 particle size is expected to vary similarly (Phani *et al.,* 2000).

Ultra Violet Spectroscopy

Fig. 2 shows that the exhibit UV-Vis spectrophotometer of synthesized Cd-TiO_2 nanocomposite powder by using solgel method. The Cd-TiO_2 nanocomposite growth phase plays an important role in nanocomposite synthesis process. The wide peak was located between 350nm for Cd-TiO_2 nanocomposite powder.

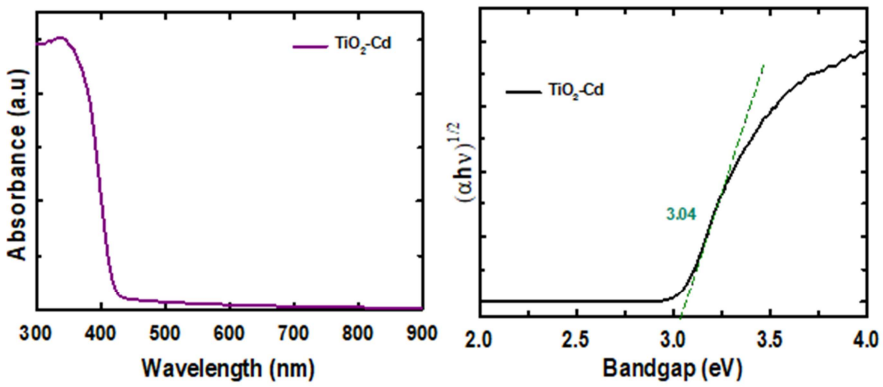

Fig. 2. The UV image of Cd-TiO_2 nanocomposite.

The absorbance of Cd-TiO_2 nanocomposite that was gradually increased after indicates gradual increase of nanocomposite. Finally the result shows that the UV-visible absorption spectrum of Cd-TiO_2 nanocomposite shows an absorption onset at 350n m (band gap = 3.04eV)

Fourier Transform Infrared Spectroscopy

Several vibration bands of the Cd-TiO_2 Nanocomposite can be observed from 4000 to 500cm^{-1} as shown in Fig. 3. In the higher energy region, the broad peak located at around 3638cm^{-1} can be consigned to the stretching vibrations band observed at O-H bond in the carboxyl group (Zhu *et al.,* 2016). The bands observed for the C-N bond at 1202cm^{-1} and 1126·cm^{-1} agrees to the stretching vibrations of the aliphatic amines and aromatic respectively.

The peak at 531 cm^{-1} agrees to anatase phase of TiO_2. The decrease in conduction elsewhere 417cm^{-1} is attributed to Ti-O stretching vibration and Ti-O-Ti lattice (Reza *et al.,* 2013). The FTIR spectral results showed the possible interactions of the Cd-TiO_2 Nanocomposite, which might be responsible for the stabilization of the nanocomposite (Zhu *et al.,* 2016).

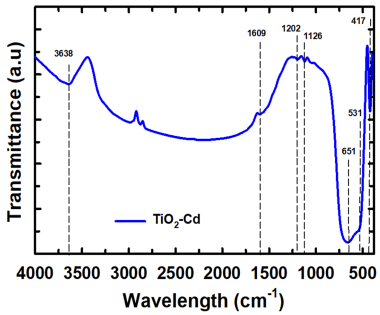

Fig. 3. FTIR image of Cd-TiO_2 Nanocomposite.

Scanning Electron Microscopy-EDAX

SEM has been used to learn the morphological analysis of the synthesised Cd-TiO_2 Nanocomposite. The SEM images of Cd-TiO_2 Nanocomposite are given in Fig. 4, respectively, and from which the average size of the Cd-TiO_2 Nanocomposite are establish in the range of 35nm. Cd-TiO_2 Nanocomposite shape such as spherical shape and then crystalline nature.

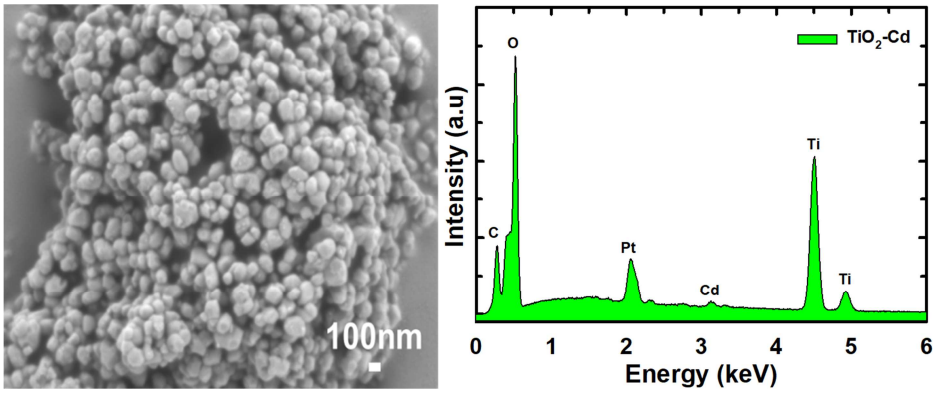

Fig. 4. The SEM image of Cd-TiO_2 Nanocomposite.

The purity of the synthesized Cd-TiO_2 Nanocomposite have been confirmed from the energy-dispersive X-ray (EDAX) spectra, which are shown in Figs 4 respectively and then C, O, Ti, Cd, Pt element are present in Cd-TiO_2 Nanocomposite. The weight percentage of Cd is 5.8%, Ti is 51.03%, C is 5.13% and O is 31.75% in Cd-TiO_2 Nanocomposite as shown in Fig. 4. The doping in Cd nanocrystals is also confirmed from the EDAX spectra. No other additional impurity peak is create in the spectra, which shows the purity of the prepared nanocrystals.

BET Surface Area Analysis

Fig. 5 shows that the N_2 adsorption-desorption isotherms and BJH pore size distribution of Cd-TiO_2 nanocomposites. The N2 adsorption-desorption isotherms of the as-prepared Cd-TiO_2 nanocomposites demonstration type IV characteristics, which is one of the main characteristics of mesoporous materials. Major pore size distribution of Cd-TiO_2 nanocomposites is ranged from 2.24nm. The BET surface area of the prepared Cd-TiO_2 nanocomposites pore volume was 0.01cm^3/g.

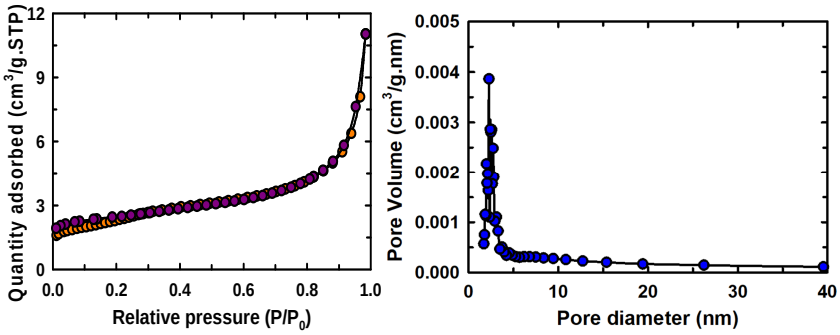

Fig. 5. The BET image of Cd-TiO_2 Nanocomposite.

The surface area of Cd-TiO_2 nanocomposites is calculated to be 8.1 m2 g^{-1} built on the BET model. The surface area of BET and mesoporous structure improve the Photo generated electrons and holes toward contribute now photocatalytic activity and deliver more channels on behalf of water molecule to go through, which is important to complete high water and photo reduction efficacy (Zhang *et al*., 2018).

Antibacterial Activity

The antibacterial activity of synthesized Cd-TiO_2 nanocomposite have been investigated against Gram-negative bacteria by the well diffusion method (Das *et al*., 2010; Das *et al*., 2012; Das *et al*., 2011; Das *et al*., 2013). The prepared solution with different concentrations (such as 25, 50, 75, 100µl) of Cd-TiO_2 nanocomposite are placed in the broth against *Pseudomonas* as shown in fig. 6, respectively. Here, the standard antibiotic ampicillin is used as a reference, whereas distilled water is used as a control. The zone of inhibition (ZOI) on the bacterial growth has been observed as shown in fig. 6 respectively, and recorded after 24 h of incubation.

Fig. 6. Antibacterial activity image of Cd-TiO_2 Nanocomposite.

The diameter of the ZOI has been measured using a measuring ruler. The Cd-TiO_2 nanocomposite showed (Fig. 6) antibacterial activity when tested against the pathogens only gram negative bacteria such as *Pseodomonous*. The zone of minimum inhibition concentration was measured in a range of 20mm in 25µl and 30mm in 100µl.

Conclusion

We have synthesised high purity bulk single phase Cd-TiO_2 nanocomposite powder from Sol-Gel technique. The formation of this single phase has been confirmed by X-ray diffraction for the crystallite size is calculated and found to be Scherrer formula applied to the three highest peak such as 27.1°, 36.0°, 54.5° orientation which is the maximum reflection of the rhombohedral structure of Cd-TiO_2 nanocomposite.

The particle size of Cd-TiO_2 nanocomposite in 35nm. The UV-visible absorption spectrum of Cd-TiO_2 nanocomposite shows an absorption onset at 350n m (band gap = 3.04eV). The SEM image shows that the Cd-TiO_2 Nanocomposite shape such as spherical shape and then crystalline nature. The purity of the synthesized Cd-TiO_2 Nanocomposite have been confirmed from the energy-dispersive X-ray (EDAX) spectra and then C, O, Ti, Cd, Pt element are present in Cd-TiO_2 Nanocomposite. The weight percentage of Cd is 5.8%, Ti is 51.03%, C is 5.13% and O is 31.75% in Cd-TiO_2 Nanocomposite.

BET image shows that the major pore size distribution of Cd-TiO2 nanocomposites is ranged from 2.24nm. The BET surface area of the prepared Cd-TiO2 nanocomposites pore volume was 0.01cm^3/g.

The surface area of Cd-TiO2 nanocomposites is calculated to be 8.1 m^2g^{-1} built on the BET model. The Cd-TiO_2 nanocomposite showed that the antibacterial activity when tested against the pathogens only gram negative bacteria such as *Pseodomonous*. The zone of minimum inhibition concentration was measured in a range of 20mm in 25µl and 30mm in 100µl.

Reference

Azam A, Ahmed AS, Oves M, Khan MS, Habib SS, Memic A. 2012. Antimicrobial activity of metal oxide nanoparticles against Gram-positive and Gram-negative bacteria: a comparative study. International Journal of Nanomedicine **7,** 6003-6009.

Chen W, Sun X, Weng D. 2006. Morphology control of titanium oxides by tetramethyl ammonium cations in hydrothermal conditions. Materials Letters **60,** 3477- 3480.

Das R, Gang S, Nath SS, Bhattacharjee R. 2012. Preparation of linoleic acid-capped silver nanocrystals and their antimicrobial effect. IET Nanobiotechnol **6,** 81-5.

Das R, Gang S, Nath SS. 2011. Preparation and antibacterial activity of silver nanocrystals. J Biomater Nanobiotechnol **2,** 472-5.

Das R, Nath SS, Chakdar D, Gope G, Bhattacharjee R. 2010. Synthesis of silver nanocrystals and their optical properties. J Exp Nanosci **5,** 357-62.

Das R, Saha M, Hussain SA, Nath SS. 2013. Silver nanocrystals and their antimicrobial activity on a few bacteria. BioNanoSci **3,** 67-72.

Demir R, Okur S, Seeker M. 2012. Electrical characterization of CdS nanocrystals for humidity sensing applications. Ind. Eng. Chem. Res. **51(8),** 3309-3313.

Dislich H. 1993. Sol. Gel Technology for Thin Films, Fibers, Preforms, Electronics and Speciality Shapes. edited by L. C. Klein (Noyes Publications, Prak Ridge, N **5,** 50.

Fades BD, Zelinski BJ, Uhlmann DR. 1993. Ceramic. Films and Coatings. edited by J. Wachtmann and JR. A. Haber (Noyes Publications, Park Ridge, NJ **2,** 224.

Giovanni M, Tay CY, Setyawati MI, Xie J, Ong CN, Fan R, Yue J, Zhang L, Leong DT. 2015. Toxicity profiling of water contextual zinc oxide, silver, and titanium dioxide nanoparticles in human oral and gastrointestinal cell systems. Environ. Toxicol **30,** 1459-1469.

Han Y, Li G, Zhang Z. 2006. Synthesis and optical properties of rutile TiO_2 microspheres composed of radically aligned nanorods. Journal of Crystal Growth **295,** 50-53.

Li L, Yang X, Gao J, Tian H, Zhao J, Hagfeldt A. 2011. Highly efficient CdS quantum dot-sensitized solar cells based on a modified polysulfide electrolyte. J Am Chem Soc **133,** 8458-8460.

Malarkodi C, Chitra K, Rajeshkumar S, Annadurai G. 2013. Novel eco-friendly synthesis of titanium oxide nanoparticles by using *Planomicrobium* sp. and its antimicrobial evaluation. Der Pharmacia Sinica **4(3),** 59-66.

Pelaez M, Nolan NT, Pillai SC, Seery MK, Falaras P, Kontos AG, Dunlop PSM, Hamilton JWJ, Byrne JA, OShea K. 2012. A Review on the Visible Light Active Titanium Dioxide Photocatalysts for Environmental Applications. Appl. Catal. B Environ **125,** 331-349.

Pettit RB, Ashley CS, Reedand ST, Brinker CJ. 1993. Sol. Gel Technology for Thin Films, Fibers, Preforms, Electronics and Speciality Shapes. edited by L. C. Klein (Noyes Publications, Prak Ridge, NJ **2(2),** 80.

Phani AR, Passacantando M, Santucci S. 2000. Synthesis and characterization of cadmium titanium oxide powders by sol-gel technique**.** Journal Of Materials Science **35,** 5295 - 5299.

Qian J, Yan S, Xiao Z. 2012. Electrochemical biosensor based on CdS nanostructure surfaces. J Colloid Interface Sci **51,** 3309-3313.

Reza M, Abdizadeh H. 2013. Effects of acid catalyst type on structural, morphological, and optoelectrical properties of spin-coated TiO_2 thin film. Phys B Phys Condens Matter **413,** 40-46.

Rzigalinski BA, Strobl JS. 2009. Cadmium-containing nanoaprticles: perspectives on pharmacology and toxicology of quantum dots. Toxicology and Applied Pharmacology **238 (3),** 280-288.

Samuela V, Pasrichab R, Ravi V. 2005. Synthesis of nanocrystalline rutile. Ceramics International **31,** 555-557.

Tabatabaee M, Baziaria P, Nasirizadeh N, Dehghanizadeh H. 2013. Synthesis of CdS nanocrystals by sonochemical reaction using thioasetamide as S2– reservoir and in the presence of a neutral surfactant, dyeing of cotton fabric and study of antibacterial effect on cotton fabric. Adv Mater Res **2,** 622-623.

Umebayashi T, Yamaki T, Tanaka S, Asai K. 2003. Visible light-induced degradation of methylene blue on S-doped TiO_2. Chem. Lett **32,** 330-331.

Vanaja M, Rajeshkumar S, Paulkumar K, Gnanajobitha G, Malarkodi C, Annadurai G. 2013. Photosynthesis and characterization of silver nanoparticles using stem extract of *Coleus aromaticus*, International Journal of Materials and Biomaterials Applications **3(1),** 1-4.

Zare M, Namratha K, Byrappa K, Surendra DM, Yallappa S, Hungund B. 2018. Surfactant assisted solvothermal synthesis of ZnO nanocrystals and study of their antimicrobial and antioxidant properties. J Mater Sci Technol **34,** 1035-1043.

Zhang H, Wang X, Li N, Xia J, Meng Q, Ding J, Lu J. 2018. Synthesis and characterization of TiO_2/ graphene oxide nanocomposites for photoreduction of heavy metal ions in reverse osmosis concentrate. RSC Advances ***8*(60),** 34241-34251.

Zhu X, Kumari D, Huang M, Achal V. 2016. Biosynthesis of CdS nanoaprticles through microbial induced calcite precipitation. Materials and Design **98,** 209-214.